On the Phase Transition between Quartz and Coesite

By

Katsumi YASKAWA

Geological and Mineralogical Institute, University of Kyoto

(Received June 15, 1963)

Abstract

In case of the synthesis of coesite by means of the anvil type apparatus, it was generally found a zonal structure in the thin discoidal products. The peripheral ring was made of quartz only and its inner region abounded in fine coesite crystals. The diameter of the latter became greater with increase of the load pressure. This suggests the existence of a pressure gradient along the radius of the specimen which was compressed between anvils. The relation between the radius of the quartz-coesite boundary and the applied load pressure was precisely investigated, and it was made clear that the pressure produced in the specimen decreased linearly from the centre to the edge. In the Part I theoretical explanations are offered in view points of elasticity and plasticity. The transformation of quartz to coesite and the reverse one are discussed, especially in connection with the pressure gradient, on the basis of experiments described in the Part II.

Part I

Experiments and Considerations on the Stress Distribution in the Material Compressed between Anvils

Introduction

In 1937, BRIDGMAN first designed the so-called anvil-type apparatus for the purpose of studying shearing phenomenon under high pressure[1]. The recent development of hard materials made him possible to modify this apparatus[2] by which he was able to generate pressures up to 100 kb. This apparatus consisted of two "Carboloy anvils" held in compression by steel binding rings as shown in Fig. 1. Regarding its characteristics, BRIDGMAN[1] described it as follows: "To a very rough approximation the material under investigation might be thought of as occupying a central chamber surrounded by a narrow channel through which it is being squeezed out, the friction on the face of the annulus holding in check the expulsive tendency of the approximately hydrostatic pressure in the chamber". His conclusion was

that the confining annulus at the edge
possessed a width of only 3% or less of
the total radius.

GRIGGS and KENNEDY[3] improved
BRIDGMAN's apparatus for the experi-
ments under higher pressure and tem-
perature. They agreed with BRIDGMAN's
conception that the stress system inside
the materials compressed by a pair of
anvils should be hydrostatic except for a
thin peripheral region which is less than
5% of the radius of the anvil. As this
type of anvil was convenient to syn-
thesize materials under high pressures,
it became more and more popular and
many interesting results were obtained
using the same kind of equipment[4].

Fig. 1. Schematic diagram of the
anvil type pressure apparatus
designed by Bridgman.

This type of high pressure apparatus, however, has some disadvantages
such as; (1) the amount of specimen produced in one run is very small,
(2) the materials, of which piston holders and pushers are made, rapidly
lose their mechanical strength when the temperature reaches 700°C and it
becomes impossible to continue the experiment at temperatures higher than
this. (3) Notwithstanding BRIDGMAN's conclusion that the pressure in the
anvils is almost hydrostatic, actually the pressure is not hydrostatic, and
consequently its distribution is considered so complicated to be analyzed that
it is hardly possible for us to know the accurate pressure applied on each
part of the specimen.

Among these disadvantages, the first one can be solved by making a
recess on the surface of the anvil which can accomodate a large amount of
specimen as shown in Fig. 2. BRIDGMAN[2] tried this apparatus, however, to
find the experimental results unsuccessful, because the anvils would lose
their strength once they had the recess. As for the second point, there had
been no hope without finding better materials for the piston holders and
pushers until, as HALL reported[5], a new equipment improved by BUNDY on
the method of heating appeared. This new model is called a "saucer"
after its shape (Fig. 3). As the author of the paper does not give any
description on the capability of this apparatus, we can not know the details
of it, but it is supposed that considering from the complicated design the
apparatus is not handy to carry out the experiment. The third one is the
most important point to discuss the phase equilibrium relationship of the
specimen produced under high pressure and temperature, and the accurate
pressure distribution on the surface of the anvil must be estimated in either
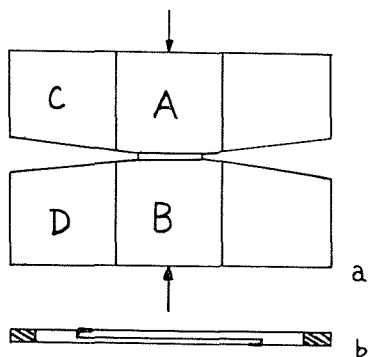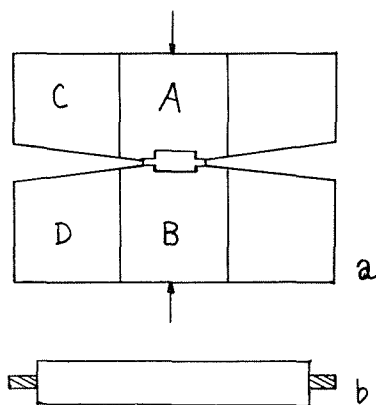theoretical or experimental way. If this point is settled, the anvil type

Fig. 2. Modified type of the anvil with a recess on the surface (after Bridgman).
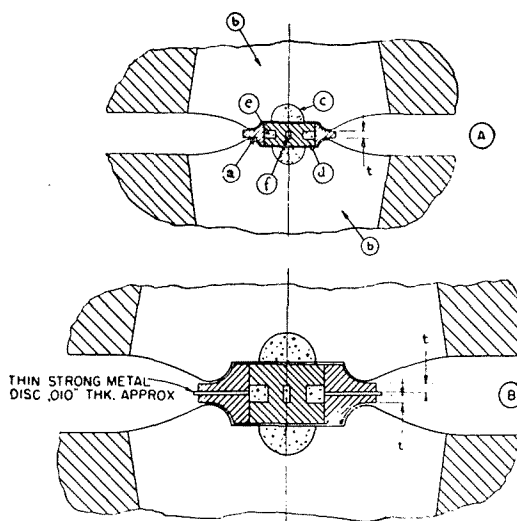

Fig. 3. Saucer type anvils (after Bundy).

apparatus would be one of the best ones for the high pressure experiment as mentioned already. In this paper, a theoretical consideration on the pressure distribution of the anvil is reported, referring to some experimental facts obtained by the author.

Apparatus

In the present study was used the modified type pressure apparatus of GRIGGS and KENNEDY shown in the schematic diagram of Fig. 4 and Plate 6-a. This apparatus consists of three main parts; the anvils, the press and the furnace. A pair of pistons, piston holders and pushers form the anvils. The material, of which the pistons are made, is tungsten-carbide. Totanloy G3 (WC 83-88%, Co binder 7-10%) pistons are used for the experiments of relatively low pressures (up to 30 kb), and Totanloy GF (WC 89-92%, Co binder 3-5%) for the experiments of higher pressures (up to 50 kb). The diameter of the flat surface of the pistons on which the specimen is charged varies from 6 mm to 12 mm and the surface is finished to be perpendicular to the direction of the applied force generated by the press.

The apex angle of the cone, 2θ, was chosen to be about 104° by the following reason. If a compressional force P is acting on the surface of a semi-infinite body along the z-axis (Fig. 5), the radial and the tangential components of the normal stress expressed in the polar co-ordinate (σ_r and σ_t in Fig. 5) are given by the equations
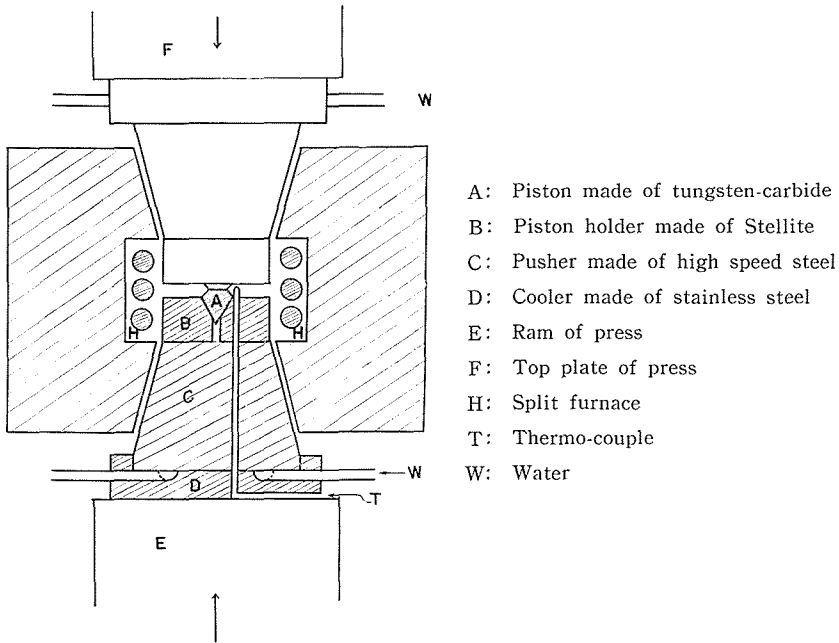
A: Piston made of tungsten-carbide

B: Piston holder made of Stellite

C: Pusher made of high speed steel

D: Cooler made of stainless steel

E: Ram of press

F: Top plate of press

H: Split furnace

T: Thermo-couple

W: Water

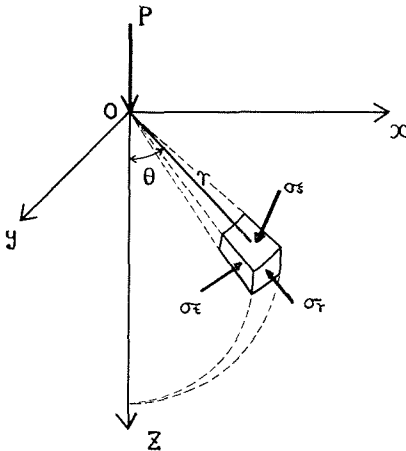Fig. 4.　Schematic diagram of the anvils which were used in the present study.

Fig. 5. Configuration of stresses worked on a semi-infinite solid illustrated by the polar co-ordinate.

$$\sigma_r = -\frac{3P}{2\pi r^2}\left\{(2-\mu)\cos\theta - \frac{1-2\mu}{2}\right\},$$

$$\sigma_t = \frac{(1-2\mu)P}{2\pi r^2}\left\{\cos\theta - \frac{1}{1+\cos\theta}\right\},$$

where μ is the Poisson's ratio. If the value of θ is so chosen as to make either $\frac{1-2\mu}{2(2-\mu)}$ or $\frac{1}{1+\cos\theta}$ equal to $\cos\theta$, σ_r or σ_t will become naught. Because the piston made of tungsten-carbide is considered to be almost ideally rigid body, σ_r is naught on a cone whose apex angle is equal to $2\cos^{-1}\frac{1}{7}$ $(\fallingdotseq 160°)$, μ being assumed to be 0.25. Therefore, σ_r is negative, that is, compressional inside of this cone, and is tensional outside of it. On the other hand σ_t may be naught on a cone, the angle of which is equal to

$2\cos^{-1}\frac{\sqrt{5}-1}{2}$ ($\fallingdotseq 103°40'$). This result shows that σ_t acts as a compression outside of this cone, whereas it acts as a tension inside of this. Thus, there is no stress worked on the direction perpendicular to the radius of the cone and no change of sign of σ_r inside of the cone, and so this piston seems to have the most stable shape under pressure.

The lower half of the piston whose shape is a 60° cone is buried in the holder. If the angle of the cone is sharper, the compression due to the piston holder which gives more strength to the piston increases. However, if the angle of the cone is too sharp, the piston would act as a wedge piercing into the holder to break it. A 60° cone seems to be the best shape. A thin copper plate inserted in the gap between the piston and the holder is useful to give the better contact on the both surfaces.

Although several kinds of steel were tried for the holder, Mitsubishi stellite D2 was found to be one of the best materials because of its high hardness and strength at high temperatures. A small hole of 3 mm in diameter is drilled through the centre of the each holder (Fig. 4) for the advantage of pushing out the piston when it is replaced by a new one. The lower holder has another hole which runs through the lower pusher to the bottom of it. A Pt–PtRd thermo-couple is set through this hole to measure the temperature of the specimen.

High speed steel of grade 2 is used to make the pusher and it is designed to have larger area at the bottom than the top.

The press is shown in Plate 6–a. On the top of the press there is a screw indicated by A. B is a 30 ton oil jack which is driven by a motor D. The pressure is kept constant by means of a relay C electrically connected with the pressure gauge.

The maximum pressure applied on the specimen by this apparatus is 50 kb at room temperature and a little less than 20 kb at 800°C. Pressures can be known from the applied force divided by the area of the flat surface of the piston.

Heating device is shown in Fig. 4. The heating elements are Tecorundum (SiC). The temperature of the specimen is measured by a Pt–PtRd thermo-couple inserted in the hole through the lower piston holder and the pusher as stated already. The distance from the centre of the specimen to the thermo-couple is about 10 mm and the correction of the temperature is necessary to know the accurate temperature of the specimen in the anvils. The temperature of the furnace is automatically controlled by a temperature regulator to keep it constant during heating, the fluctuation of the temperature being less than 10°C.

Experiments and results

The specimen used in the experiment was Merk's silica gel moisted with

water. This was sandwiched by two sheets of gold foils and inserted be-
tween the pistons. Then pressures and temperatures of various combinations
were applied on the specimen for several hours. After the treatment which
seemed to be long enough to attain the equilibrium state, the pressure and
temperature was released as quickly as possible to establish the quenched
state.

The product thus obtained had the form of a thin disc whose thickness
was slightly greater at the centre. Whenever the experimental conditions
of pressure and temperature were high enough to produce coesite, the
product possessed a concentric zonal structure, separating the product into
two parts, that is, the central part and the outer ring. The central part
was always more transparent than the outer ring which was rather smoky
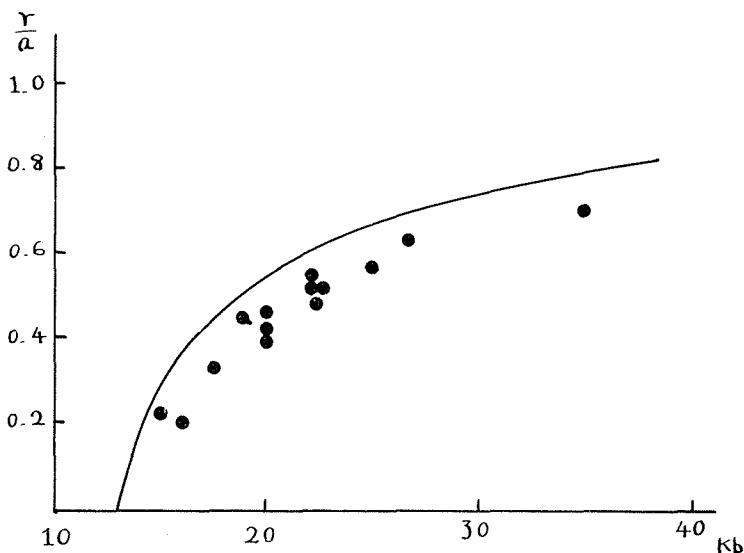(Plate 6-b). The X-ray analyses showed that the central part was an

Fig. 6. The relation between the loaded mean pressure
and the radius of coesite region.

aggregate of fine-grained coesite and trace quartz, and the outer ring that
of quartz. The diameter of the central part increased with the increase of
the applied pressure if the temperature was kept constant. This zonal
structure disappeared at pressure lower than a certain critical value P_c
below which all of the products were fine-grained quartz. Denoting the
radius of the whole disc as a and that of the central part as r respectively,
the relation of $\frac{r}{a}$ to the applied pressure was found as shown in Fig. 6, in

which series of dot represents the rela-
tion observed and the solid line theoreti-
cal (refer to p. 135). This relation can
be approximately drawn as $\dfrac{r}{a}=1-\dfrac{P_c}{P}$.
It was also the experimental fact that
the critical pressure P_c was a simple
function of temperature (t) and repre-
sented by the following equation as
shown in Fig. 7, $P_c=At+B$, where A and
B are constant.

Theoretical consideration of the stress distribution in the specimen.

As stated already, BRIDGMAN[1] showed
that a specimen compressed between a
pair of anvils was subjected to hydro-
static pressure except for a narrow peri-
pheral region. In his consideration the
deformation of the anvil is assumed to
be almost the same as that of semi-infinite
elastic body under the existence of hy-
drostatic pressure. However, there are
two difficulties to approve this conside-
ration. The first one is that concerning
the shape of the resulted specimen resem-
bling a convex lens. BRIDGMAN con-
sidered that this shape was the replica
of the surface of the anvil which had
been deformed into the shape of lens
during the compression. However, if the
high rigidity of tungsten-carbide is
taken into account, it is more plausible

Fig. 7. Schematic diagram of the
quartz-coesite equilibrium relation.
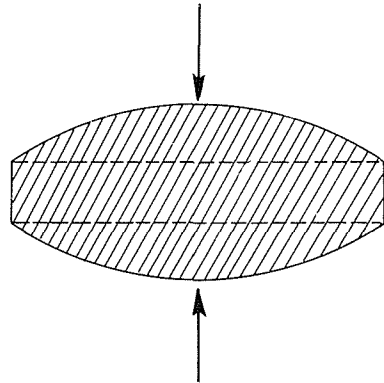
Fig. 8. Schematic diagram of the
shape of specimen compressed by
the loaded pressure P.

that the anvil has never been deformed, but the specimen which was keep-
ing the disc shape of uniform thickness during the compression has recovered
its free shape resembling a convex lens (Fig. 8) as the applied pressure was
released. The second is that: If the lens shape of the specimen is due to
the deformation of the anvil as stated by BRIDGMAN which is idealized as
the deformation of a semi-infinite solid, we cannot consider that the pres-
sure is applied uniformly over the specimen owing to the following reason.

The vertical depression at the surface of semi-infinite elastic body
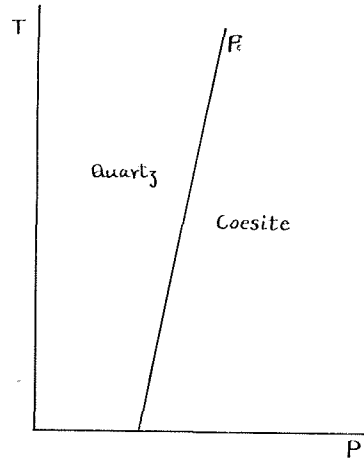subjected to uniformly distributed pressure P are given by the following

equations (BEZUKHOV, 1953, p. 212, in Japanese; TIMOSHENKO, 1934, p. 333):

$$w_0 = \frac{2(1-\mu^2)}{\pi aE} P,$$

$$w_a = \frac{4(1-\mu^2)}{\pi^2 aE} P,$$

where w_0 and w_a are the depressions at the centre and at the edge respectively, μ Poisson's ratio, E Young's modulus and P load pressure. So we have the ratio $\frac{w_0}{w_a} = \frac{\pi}{2} \doteqdot 1.57$. Next we take up a hemispherical pressure distribution over the same circular area. In this case we have

$$\dot{w}_0 = \frac{3(1-\mu^2)}{4\pi a} P,$$

$$w_a = \frac{3(1-\mu^2)}{8\pi a} P,$$

and then we get $\frac{w_0}{w_a} = 2$. Therefore we can know the disc would be lens-shaped in both cases, and the ratio of the thickness at the centre to that at the edge of the lens was $0.01/0.002 = 5$ as obtained by BRIDGMAN. This value would be much greater than that in the case of hemispherical distribution in which the ratio should be 2 as mentioned above.

(i) *Stress distribution in the specimen treated as an elastic body.*

From the experimental conditions of the study, the stress distribution in the discoidal specimen is considered to be symmetrical with respect to the axis of the disc. There are a few solutions regarding the stress distribution in a symmetrically deformed circular cylinder[6], but as they are not applicable to our case, the author has tried to find the suitable solution as follows:

If the stress distribution is assumed to be axially symmetrical, the equilibrium state is represented by the equations

$$\left.\begin{array}{l} \dfrac{\partial \sigma_r}{\partial r} + \dfrac{\partial \tau_{rz}}{\partial z} + \dfrac{\sigma_r - \sigma_\theta}{r} = 0, \\[2mm] \dfrac{\partial \tau_{rz}}{\partial r} + \dfrac{\partial \sigma_z}{\partial z} + \dfrac{\tau_{rz}}{r} = 0, \end{array}\right\} \tag{1}$$

where σ_r, σ_θ and σ_z are the normal components of stress in the cylindrical co-ordinate and τ_{rz} is its shearing component. If we substitute the well-known relations of

$$\left.\begin{array}{ll} \varepsilon_z = \dfrac{\partial w}{\partial z}, & \varepsilon_r = \dfrac{\partial u}{\partial r}, \\[2mm] \varepsilon_\theta = \dfrac{u}{r}, & \gamma_{rz} = \dfrac{\partial w}{\partial r} + \dfrac{\partial u}{\partial z}, \end{array}\right\} \tag{2}$$

$$\sigma_r = 2G\varepsilon_r + \frac{2\mu G}{1-2\mu}\Theta,$$

$$\sigma_\theta = 2G\varepsilon_\theta + \frac{2\mu G}{1-2\mu}\Theta,$$

$$\sigma_z = 2G\varepsilon_z + \frac{2\mu G}{1-2\mu}\Theta,$$

$$\tau_{rz} = G\gamma_{rz},$$

(3)

into equation (1), the following equations of equilibrium expressed in terms of the displacement[7] are obtained;

$$\frac{\partial^2 w}{\partial z^2} + \frac{1-2\mu}{2(1-\mu)}D\frac{\partial w}{\partial r} + \frac{1}{2(1-\mu)}\frac{\partial}{\partial z}Du = 0,$$

$$D^2 u + \frac{1-2\mu}{2(1-\mu)}\frac{\partial^2 u}{\partial z^2} + \frac{1}{2(1-\mu)}\frac{\partial^2 w}{\partial r\partial z} = 0,$$

(4)

where ε_r, ε_θ and ε_z are unit elongations of the specimen and γ_{rz} is unit shearing strain in the cylindrical co-ordinate; u, v and w are three components of the displacement in r-, θ- and z-directions; Θ is the volume expansion denoted by the relation $\Theta = \varepsilon_r + \varepsilon_\theta + \varepsilon_z$; G is the shear modulus; μ is Poisson's ratio; D is a differential operator defined as

$$D = \left(\frac{\partial}{\partial r} + \frac{1}{r}\right),$$

and

$$D^2 = \frac{\partial}{\partial r}\left(\frac{\partial}{\partial r} + \frac{1}{r}\right) = \left(\frac{\partial^2}{\partial r^2} + \frac{1}{r}\frac{\partial}{\partial r} - \frac{1}{r^2}\right).$$

By eliminating w in the equations (4), the following partial differential equation of the 4th order is obtained,

$$\left(\frac{\partial^2}{\partial z^2} + D^2\right)^2 u = 0.$$

(5)

The solution of this equation is given by the product of the following $R(r)$ and $Z(z)$;

$$R(r) = \begin{cases} I_1(ar) + carI_2(ar) \\ K_1(ar) + carK_2(ar), \end{cases} \quad Z(z) = \begin{cases} \sin az \\ \cos az, \end{cases}$$

(6)

or

$$R(r) = \begin{cases} J_1(ar) + karJ_2(ar) \\ N_1(ar) + karN_2(ar), \end{cases} \quad Z(z) = \begin{cases} \sinh az \\ \cosh az, \end{cases}$$

(7)

where $I_n(x)$, $K_n(x)$, $J_n(x)$ and $N_n(x)$ are cylindrical functions. From these solutions and the equations (4), it is expected that $w(r, z)$ takes the form of

$$R(r) = \begin{cases} I_0(ar) + c'arI_1(ar) \\ K_0(ar) + c'arK_1(ar), \end{cases} \quad Z(z) = \begin{cases} \sin az \\ \cos az, \end{cases}$$

(8)

or $\qquad R(r) = \begin{cases} J_0(ar) + k'arJ_1(ar) \\ N_0(ar) + k'arN_1(ar), \end{cases} \quad Z(z) = \begin{cases} \sinh az \\ \cosh az. \end{cases}$ $\qquad$ (9)

If we take the axis of symmetry as z-axis and the middle point of the segment of z-axis contained between the upper and the lower anvils as the origin of the co-ordinate (Fig. 9), the boundary conditions are given as follows;
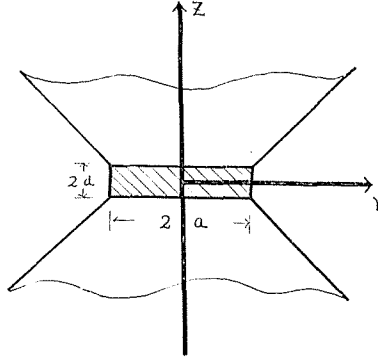

Fig. 9. Position of co-ordinate taken on the anvils.

$$w(r, 0) = 0,$$ $\qquad$ (10)

$$w(r, \pm d) = \pm f(r),$$ $\qquad$ (11)

$$u(0, z) = 0,$$ $\qquad$ (12)

$$\sigma_r(a, z) = 0,$$ $\qquad$ (13)

$$\sigma_r(0, z) = \sigma_\theta(0, z),$$ $\qquad$ (14)

$$\pi a^2 p = 2\pi \int_0^a \sigma_z(r, d) \cdot r \cdot dr,$$ $\qquad$ (15)

where $\pi a^2 p$ is the force applied along z-axis. The solution which is convergent at the origin and satisfies the boundary conditions (10) and (11) is given by the product of (9), that is;

$$w(r, z) = \sum_{n=0}^{\infty} a_n \sinh\left(\alpha_n \frac{z}{a}\right)\left\{J_0\left(\alpha_n \frac{r}{a}\right) + k'arJ_1\left(\alpha_n \frac{r}{a}\right)\right\},$$ $\qquad$ (16)

where $a = \dfrac{\alpha_n}{a}$ and α_n is defined by the equation $J_1(\alpha_n) = 0$.

Now assuming $f(r) = f_1(r) + f_2(r)$, we can expand $f_1(r)$ with $J_0\left(\alpha_n \dfrac{r}{a}\right)$ and $f_2(r)$ with $arJ_1\left(\alpha_n \dfrac{r}{a}\right)$, that is;

$$f_1(r) = \frac{2}{a^2}\int_0^a f_1(\rho)\rho d\rho + \frac{2}{a^2}\sum_{n=1}^{\infty}\frac{J_0\left(\alpha_n\frac{r}{a}\right)}{J_0{}^2(\alpha_n)}\int_0^a f(\rho)J_0\left(\alpha_n\frac{\rho}{a}\right)\rho d\rho ,\qquad (17)$$

$$f_2(r) = \frac{2}{a^2}\sum_{n=1}^{\infty}\frac{\alpha r J_1\left(\alpha_n\frac{r}{a}\right)}{J_2{}^2(\alpha_n)}\int_0^a f_2(\rho)J_1\left(\alpha_n\frac{\rho}{a}\right)d\rho .\qquad (18)$$

From the equations (16), (17), (18) and $w(r, d) = f(r) = f_1(r) + f_2(r)$, we obtain the following result;

$$w(r,z) = \frac{2}{a^2}\sum_{n=1}^{\infty}\frac{\sinh(\alpha z)}{\sinh(\alpha d)J_0{}^2(\alpha_n)}\left\{F_1(\alpha_n)J_0\left(\alpha_n\frac{r}{a}\right) + F_2(\alpha_n)\alpha r J_1\left(\alpha_n\frac{r}{a}\right)\right\},\qquad (19)$$

where $F_1(\alpha_n) = \displaystyle\int_0^a f_1(\rho)J_0\left(\alpha_n\frac{\rho}{a}\right)\rho d\rho ,$ \hfill (20)

$$F_2(\alpha_n) = \int_0^a f_2(\rho)J_1\left(\alpha_n\frac{\rho}{a}\right)d\rho .\qquad (21)$$

And also we obtain from the equations (4), (7) and (19);

$$u(r, z) = \frac{2}{a^2}\sum_{n=1}^{\infty}\frac{\cosh(\alpha z)}{\sinh(\alpha d)J_0{}^2(\alpha_n)}\left\{F_2\alpha r J_0(\alpha r) - [F_1 + 4(1-\mu)F_2]J_1(\alpha r)\right\} .\qquad (22)$$

The solution (22) satisfies the boundary condition (12). Putting u and w into the equations (2) and (3), we obtain the equations of the stress components;

$$\sigma_r(r, z) = -\frac{4G}{a^2}\sum_{n=1}^{\infty}\frac{\alpha\cosh(\alpha z)}{\sinh(\alpha d)J_0{}^2(\alpha_n)}\left\{[F_1 + (3-2\mu)F_2]J_0(\alpha r)\right.$$
$$\left. + \left[F_2\alpha r - \frac{F_1 + 4(1-\mu)F_2}{\alpha r}\right]J_1(\alpha r)\right\} ,\qquad (23)$$

$$\sigma_\theta(r, z) = -\frac{4G}{a^2}\sum_{n=1}^{\infty}\frac{\alpha\cosh(\alpha z)}{\sinh(\alpha d)J_0{}^2(\alpha_n)}\left\{-(1-2\mu)F_2 J_0(\alpha r) + \frac{F_1 + 4(1-\mu)F_2}{\alpha r}J_1(\alpha r)\right\},\quad 24)$$

$$\sigma_z(r, z) = \frac{4G}{a^2}\sum_{n=1}^{\infty}\frac{\alpha\cosh(\alpha z)}{\sinh(\alpha d)J_0{}^2(\alpha_n)}\left\{(F_1 - 2\mu F_2)J_0(\alpha r) + F_2\alpha r J_1(\alpha r)\right\} ,\qquad (25)$$

$$\tau_{rz}(r, z) = \frac{4G}{a^2}\sum_{n=1}^{\infty}\frac{\alpha\sinh(\alpha z)}{\sinh(\alpha d)J_0{}^2(\alpha_n)}\left\{F_2\alpha r J_0(\alpha r) - [F_1 + 2(1-\mu)F_2]J_1(\alpha r)\right\} .\qquad (26)$$

According to the boundary condition (13), $\sigma_r(a, z)$ must be equal to zero, that is;

$$F_1(\alpha_n) + (3-2\mu)F_2(\alpha_n) = 0 .\qquad (27)$$

And if we put $f_1(r)$ as follows,

$$f_1(r) = \frac{(3-2\mu)J_1\left(a_n\frac{r}{a}\right)f(a)}{(3-2\mu)J_1\left(a_n\frac{r}{a}\right)-rJ_0\left(a_n\frac{r}{a}\right)}, \tag{28}$$

the equation (21) will be satisfied.

Now let us put $f(r)=w_d$ (const.), and integrate σ_z according to the boundary condition (15), and we obtain the final equations for stress components ;

$$\sigma_r = \frac{4Gw_d}{a^2}\sum_{n=1}^{\infty}\frac{aS_n\cosh(az)}{\sinh(ad)J_0^2(a_n)}\left\{ar-\frac{1-2\mu}{ar}\right\}J_1(ar), \tag{29}$$

$$\sigma_\theta = \frac{4(1-2\mu)Gw_d}{a^2}\sum_{n=1}^{\infty}\frac{aS_n\cosh(az)}{\sinh(ad)J_0^2(a_n)}\left\{-J_0(ar)+\frac{1}{ar}J_1(ar)\right\}, \tag{30}$$

$$\sigma_z = \frac{4Gw_d}{a^2}\sum_{n=1}^{\infty}\frac{aS_n\cosh(az)}{\sinh(ad)J_0^2(a_n)}\left\{3J_0(ar)-arJ_1(ar)\right\}, \tag{31}$$

$$\tau_{rz} = -\frac{4Gw_d}{a^2}\sum_{n=1}^{\infty}\frac{aS_n\sinh(az)}{\sinh(ad)J(a_0^2{}_n)}\left\{arJ_0(ar)+J_1(ar)\right\}, \tag{32}$$

where $w_d = \dfrac{a^2p}{8G\sum_{n=1}^{\infty}aS_n\coth(ad)/J_0(a_n)}$,

$S_n = \displaystyle\int_0^a\frac{\rho J_0(a\rho)J_1(a\rho)d\rho}{(3-2\mu)J_1(a\rho)-\rho J_0(a\rho)}$.

It is clear that the equations (29) and (30) satisfy the condition (14). As seen in these equations, the hydrostatic pressure does not act in any part of the specimen.

(ii) *Stress distribution in the specimen treated as a plastic body.*

In the case when a specimen behaves as a perfectly plastic body, again it is assumed that all the stress components except for σ_r, σ_θ, σ_z and τ_{rz} are zero because the stress distributions are axially symmetrical. If no body force works on the specimen, the equation of the equilibrium has the same form as in the case of a perfectly elastic body. The criterion of yielding by von MISES is

$$(\sigma_r-\sigma_\theta)^2+(\sigma_\theta-\sigma_z)^2+(\sigma_z-\sigma_r)^2+6\tau_{rz}^2 = 6K^2. \tag{33}$$

Since Hook's Law is no longer valid in the case of the deformation of a plastic body, the problem in question cannot be solved in general. However, assuming that the stress in the disc is independent of z, and also assuming that σ_r is equal to σ_θ, we get the following solution on this problem. (An analogous method was used by SIEBEL[8] on the correction of the measured compressive strength.) These assumptions can be applicable to our case because the ratio of the height to the diameter is so small that the varia-

tions of normal stress along z-axis can be neglected. On the other hand, as σ_r must be equal to σ_θ at the centre of disc lest σ_r should not become infinite as known in the equation (1), it may be expected that σ_r is not different so far from σ_θ over the disc.

Using these assumptions, the first equation (1) is reduced to the following form ;

$$\frac{\partial \sigma_r}{\partial r} = -\frac{\partial \tau_{rz}}{\partial z} .$$

Integrating this equation regarding z in the range from 0 to $2d$, we obtain

$$2d \frac{\partial \sigma_r}{\partial r} = -2mK , \tag{34}$$

where m is the coefficient of effective friction and K is defined in such a way that $\sqrt{3} K$ is identical with the tensile strength of yielding. If m is small enough to neglect τ_{rz}, the equation (33) is reduced to

$$\sigma_r - \sigma_z = \pm\sqrt{3} K . \tag{35}$$

From (34) and (35) we obtain

$$\frac{d\sigma_z}{dr} = -\frac{m}{d} K .$$

Integrating both members of this equation regarding r and using the boundary condition $\sigma_z = -\sqrt{3} K$ at $r=a$ (because $\sigma_r = 0$ at $r=a$ and σ_z is considered to be compression), we get

$$\left. \begin{aligned} \frac{\sigma_z}{K} &= -\sqrt{3} - \frac{m}{d} (a-r) , \\ \frac{\sigma_r}{K} &= -\frac{m}{d} (a-r) . \end{aligned} \right\} \tag{36}$$

PRANDTL[9] solved the stress distribution of a rectangular block compressed with rough plates, i.e.

$$\frac{\sigma_x}{K} = -c - \frac{mx}{d} + 2\sqrt{1 - \frac{m^2 z^2}{d^2}} ,$$

$$\frac{\sigma_z}{K} = -c - \frac{mx}{d} , \quad \frac{\tau_{xz}}{K} = \frac{m}{d} z ,$$

$$c = \frac{\sin^{-1} m}{m} + \sqrt{1 - m^2} .$$

These equations and the equations (36) represent the almost same relation near the edge of the disc and the block, confirming a good approximation of the equations (36).

As is known from (36), σ_z cannot take values greater than $\sqrt{3}\,K$ in absolute value, and σ_r and σ_θ are zero, if there is no friction i.e. $m=0$. If m is not zero, the thickness of the disc d is a function of the mean pressure p, being represented by the relation

$$-p = \frac{2\pi \int_0^a \sigma_z r\,dr}{\pi a^2}\ .$$

Then we get
$$d = ma \Big/ 3\Big(\frac{p}{K} - \sqrt{3}\,\Big)\ .$$

If we put $m=0.2$, $a=5$ mm, $K=7$ kb and $p=30$ kb, d becomes 0.12 mm. This value seems to be a reasonable thickness as the actual thickness is between 0.08 and 0.12 mm at the centre and between 0.02 and 0.04 mm at the edge.

Fig 10 shows the distribution of normal stress along the radius of the disc. The stress decreases as the distance from the centre increases showing the same tendency as that of elastic body. Both the radial component σ_r and the tangential component σ_θ are compression in this case, whereas they are both tension in the case of elastic body.
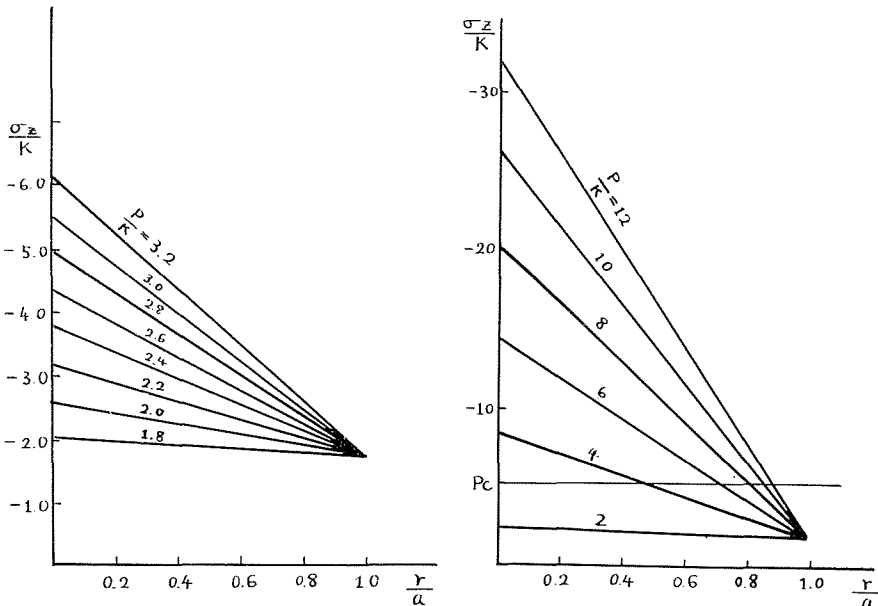

Fig. 10.   Distribution of the stress in the specimen calculated by the assumption that the specimen behaves as a plastic body.

Discussions

In Fig. 6, it does not seem for $\frac{r}{a}$ to be related to the heating tempera-
ture, although the relation with which every points of the same temperature
are connected should be the one like Fig. 11. This discrepancy is considered
that, in the quartz–coesite equilibrium curve, the ratio of pressure to tem-
perature is so large that it is difficult to know the relation between p and
$\frac{r}{a}$ more precisely and to expect a good agreement of the experimental
result with that of the theoretical consideration (Fig. 11). If the tempera-
tures in all runs of the experiments are regarded as the same temperature,
i.e. about 500°C, and if we take p_c as the transition pressure between quartz
and coesite at the temperature 500°C, the intersecting points of every curve
in Fig. 10 with the line p_c parallel to the $\frac{r}{a}$-axis show the distance from
the centre of the disc where the working pressure reaches p_c. On the basis
of the interrelationship between p and $\frac{r}{a}$ thus obtained, the curve in Fig. 6
was drawn using the value of tensile strength of quartz 7,000 kgr/cm²[10].
As all the points plotted from the experimental results are distributed along
this curve, it is reasonable to say that the stress distribution obtained in
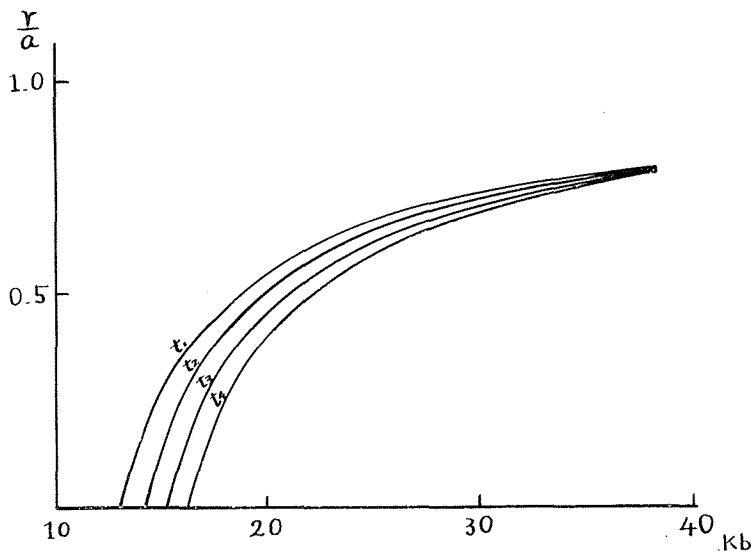the preceding section is correct.

Fig. 11. Schematic diagram of the curves of $\frac{r}{a} = f(p)$
at various temperatures.

The consideration mentioned above has been treated with the case of the disc with the free edge. The results, however, are also applicable to the case of the disc suffering from a confining pressure on its edge, that is, in the case when a metal ring or a pipe-stone gasket is used in the periphery of the specimen between the anvils. This confining pressure is considered to be constant at an equilibrium state, and then the same sort of linear relationship as that mentioned in the preceding section can be obtained with disregard of the difference of the values of σ_r at $r=a$. In Fig. 12, the schemata of the stress distribution in the case using a ring are shown. Diagram (a) in this figure shows the stress distribution in the ordinary case, and (b) is an ideal case in which m is naught inside the ring. It is regarded that the pressure acting over the discoidal specimen is hydrostatic in the case (b).
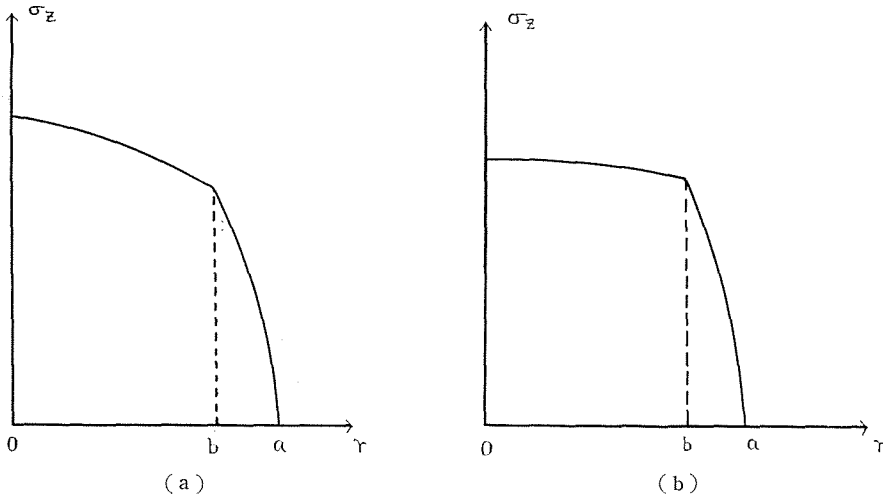

Fig. 12. The schemata of the stress distribution in the case using a ring, (a) in the ordinary case and (b) in the ideal case in which m is naught inside the ring.

BOYD and ENGLAND[11] reported an instance of experiment in which neither ring nor gasket was used. In their case coesite was distributed in the zone midway between centre and edge, and quartz at the centre and at the edge region. In the present study there are also few cases in which quartz was able to be found at the central part of coesite region of the disc. This fact may be explained by another factors from pressure gradients, e.g. temperature gradient, unflatness etc.

If there are some pressure gradients in the disc, the assumed mean pressures can be always underestimated. Nevertheless, it is said that

BRIDGMAN overestimated the pressure acting on the specimen by about 30 per cent[12]. The reason for this does not seem to be due to the gradient of pressure mentioned above. BRIDGMAN mentioned[2] that the thickness of the capsule of AgCl was thinner than that of pipe-stone (whose thickness was 0.01 in.) by 0.001 in., and pipe-stone was reduced its volume about 16% under 100 kb. He also mentioned pipe-stone ring and AgCl capsule were compressed only along the axis of disc and there was little expansion along the radius. Moreover, their compressibilities were nearly the same with each other. So that we can consider that 16% reduction of volume is due to the decrease of thickness by 16% i.e. 0.0016 in.. This shows that the pipe-stone ring was more compressed than the AgCl capsule by 6% in thickness. If we assume the areas of both ring and capsule nearly equal, the mean pressure acting on the pipe-stone ring must be higher than the mean pressure by about $1/2 \times 6/16 = 20\%$ and that the mean pressure on the AgCl capsule must be lower than the mean pressure by about 20%.

References

1) BRIDGMAN, P. W. : Am. Acad. Arts Sci. Proc., **71**, p. 387 (1937).
2) BRIDGMAN, P. W. : Am. Acad. Arts Sci. Proc., **81**, p. 165 (1952).
3) GRIGGS, D. T. and G. C. KENNEDY : Am. J. Sci., **254**, p. 722 (1956).
4) MacDONALD, G. J. F. : Am. J. Sci., **254**, p. 713 (1956).
   KHITAROV, N. N., A. B. SLURSKIY and R. V. ARSEN'YEVA : Geokhimiya, 8, p. 666 (1957).
   BOYD, F. R. and J. L. ENGLAND : J. Geophys. Research, **65**, p. 749 (1960).
   RINGWOOD, A. E. and Merreu SEABROOK : J. Geophys. Research, **67**, p. 1975 (1962).
5) HALL, H. T. : Rev. Sci. Instrument, **31**, p. 126 (1960).
6) POCHHAMMER, L. : Crelle's Jour., **81**, (1876).
   CHREE, C. : Trans. Cambridge Phil. Soc., **14**, p. 250 (1889).
   FILON, L. N. G. : Phil. Trans. Roy. Soc., London, series A, **198**, (1902).
   FÖPPL, A. and L. FÖPPL : Drang und Zwang, 2, p. 168 (1928).
   NADAI, A. : Elastische Platten, p. 315 (1925).
   TIMOSHENKO, S. : Theory of elasticity, p. 352 (1932).
7) Безухов, Н. И. : Теория Упругости и Пластичности, p. 138 (1953), (in Japanese).
8) SIEBEL, E. : Stahl und Eisen, **43**, p. 1295 (1923).
9) PRANDTL, L. : Zeits. ang. Math. Mech., **3**, p. 401 (1923).
10) ZWIKKER, C. : Physical Properties of Solid Materials, (1955).
11) BOYD, F. R. and J. L. ENGLAND : see (4).
12) KENNEDY, G. C. and P. N. LaMORI : Progress in Very High Pressure Research, John Wiley & Sons, New York, (1961).
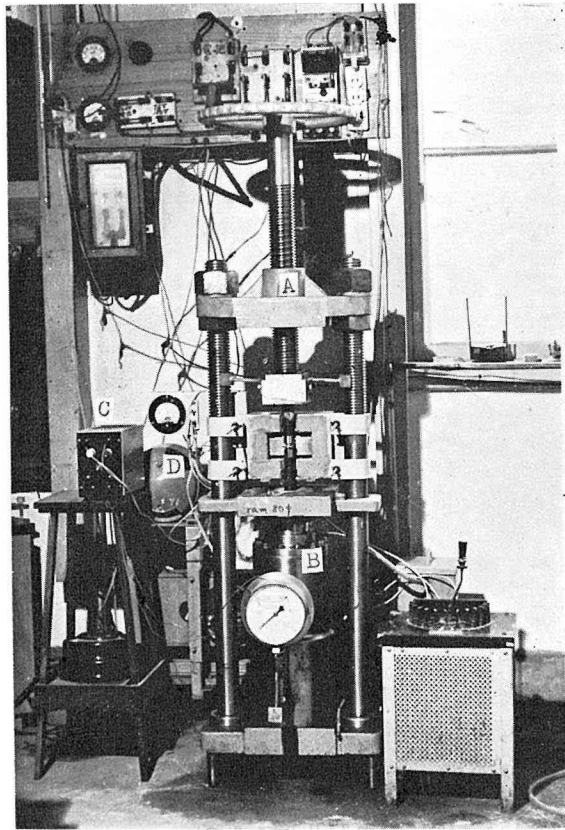
a
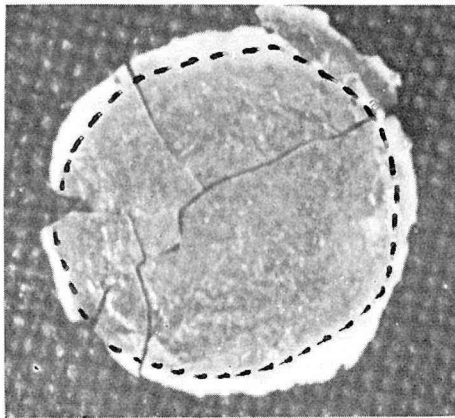
b

Part II

Transition between Quartz and Coesite

Introduction

It was 1953 when COES[1] succeeded in synthesizing a new polymorph of silica which had the density of 3.01 and the refractive indices of 1.599 for α and 1.604 for γ, and was stable against long heating in hydrofluoric acid. This dense form of silica has been called "coesite" since SOSMAN's proposal in 1954[2]. To synthesize this mineral, COES used the mixture of dry sodium metasilicate and a mineralizing agent such as diammonium phosphate, boric acid, ammonium chloride, ammonium vanadate or potassium fluoborate. This mixture was heated at a temperature between 500° and 800°C under pressures above 35 kb*. He also succeeded in the synthesis by the oxidation of silicon with silver carbonate under the same experimental conditions of temperature and pressure.

Using this new product, he made the optical and X-ray analyses. RAMSDELL[3] first studied its crystallographic properties and was followed by ZOLTAI and BUERGER[4] on the same problem, and also by KHITAROV and his co-workers[5] on the crystallographical and optical properties. One of these interesting results is concerning the optic sign. KHITAROV et al. reported that it is negative, whereas COES reported as positive.

After GRIGGS and KENNEDY[6] reported the preliminary survey, there have been a few papers concerning the P-T equilibrium relationship between coesite and quartz. For example MACDONALD[7], using the anvil-type pressure apparatus, investigated the quartz-coesite equilibrium relationship in the temperature range from 400° to 600°C, calculating the entropy and the latent heat at the formation of coesite. HALL[8] reported that coesite grew above 32 kb at 650°C, although he did not discriminate the change of transition pressure in the temperature range between 550° and 750°C, suggesting an equilibrium curve with steep gradient. This suggestion was experimentally confirmed by BOYD and ENGLAND[9] who drew a new P-T equilibrium relationship between quartz and coesite. The pressure vessel they used had the internally heating device and this made them possible to extend the range of experiment up to 1700°C in temperature and up to 40 kb in pressure. This new equilibrium curve does not agree with MACDONALD's but the magnitude of pressure obtained by the former is greater than the latter

---

* According to HALL[10] coesite has been synthesized directly from quartz without the aid of a mineralizer at pressure of 90 kb and temperature of 2000°C.

by about 10 to 20%. BOYD and ENGLAND considered that this difference was due to that of the apparatus, since they obtained the same relation with MacDONALD's when they used an anvil apparatus. They explained this phenomenon by the existence of a pressure gradient inside the sample. In the case of the anvil aparatus, there exists a pressure gradient in the sample acting as the pressure medium in the anvil apparatus because both coesite and quartz possess the high strength. Therefore the pressure acting on the sample is slightly greater than the measured value.

COES emphasized[1] that the dense polymorph of silica was so stable that any treatment to convert coesite into quartz was not successful. However, the results of investigation obtained by the author showed that this reverse transformation is possible to occur. In this paper, he will offer new experimental results of the synthesis of coesite and discuss its stability precisely.

Experimentals

As mentioned in Part I, the starting material to synthesize coesite in this study was Merk's silica gel kneaded with distilled water. In the case of the transition from coesite to quartz, pulverized coesite and silica gel mixed in the proportion of 1 : 1 was used.

These test specimens were wrapped with a thin gold foil of 0.002 mm thick and put between a pair of the anvils to be compressed by the squeezer. An external furnace was used to heat the specimen, the heating rate being 30°C/min.. After 4 or 5 hours' treatment which seemed to be long enough to establish the equilibrium state of the reaction, the applied pressure and temperature were removed as quickly as possible to quench the equilibrium state at the high temperature and pressure.

The specimen produced in this way had the shape of a disc which consisted of two parts, the inner disc and the outer ring. Very often, the inner disc was transparent and the outer ring was smoky and it was not difficult to distinguish the former from the latter even by the naked eye. Microscopic observation and X-ray analysis showed that the inner disc consisted of coesite with quartz in trace and the outer ring consisted of quartz. Plate 7-a shows an example of the discoidal specimen in which the inner disc and the outer ring are observed, and Plate 7-b is the microscopic photograph of it. X-ray powder patterns for each part of the inner disc and the outer ring were taken, their numerical values being shown in Table 1.

Results

In order to obtain the accurate P-T equilibrium relationship on the transition between quartz and coesite, the correction is necessary for the experimental results following the theoretical consideration described in Part I.

Table 1

α–quartz		coesite	
d (Å)	I/I_0	d (Å)	I/I_0
4.25	25	6.20	40
3.35	100	4.38	20
2.45	15	3.43	60
2.29	10	3.09	100
2.23	6	2.76	40
2.12	9	2.69	40
1.97	8	2.33	40
1.82	25	2.29	40
1.66	8	2.18	40
1.54	20	2.03	40
1.450	2	1.84	20
1.375	25	1.79	40
1.299	4	1.71	40
1.256	3	1.70	40
1.228	3	1.66	20
1.200	6	1.58	20
1.180	8	1.545	40
1.155	1	1.501	20
1.080	4	1.418	20
1.048	2	1.409	20
1.048	8	1.345	40
1.015	1	1.321	20
		1.285	40
		1.236	20
		1.171	20

In this correction, it seems more natural to assume that the specimen behaves as an elastic body because of the following reasons, (1) The compressive strength increases if the shape of the specimen is a thin disc, as reported by VOLAROCICH and PARKOMENKO[11]. (2) In ionic materials the compressive strength is always considerably higher than the tensile strength[12]. In an extreme case, the ratio of the compressive strength to the tensile strength reaches 20 to 1. (3) The compressive strength also depends on the nature of the crystal. In cubic metals the compressive strength of poly-crystals is higher than that of a single crystal twice or three times as much. In hexagonal metal, however, the ratio of compressive strength of poly-crystals to that of a single crystal reaches several hundreds[13].

In spite of these facts, the author corrected his results using the model

of a plastic body, because the starting material is the form of pulverized gel kneaded with water and it seems better to assume that the specimen behaves as a plastic body.

Table 2

Temperature (°C)	Pressure (kb)	Time	Results	
			centre	margin
		h m		
775	15.0	1,00	Q	Q
765	16.0	3,00	Q	Q
595	22.5	2,00	C	Q
595	20.0	4,00	C	Q
585	22.5	4,30	C	Q
580	16.0	3,00	C	Q
575	14.4	16,00	C	Q & C
575	14.0	3,40	C	Q
570	13.8	5,00	C	Q & C
560	21.0	4,00	C	Q
555	35.0	2,00	C	Q
550	35.0	1,00	C	Q
550	32.6	2,40	C	Q
550	22.5	2,15	C	Q
540	35.0	1,50	C	Q
530	18.8	1,30	C	Q & C
530	17.4	1,40	C	Q & C
500	10.0	3,15	Q	Q
495	14.0	11,00	C	Q
470	14.5	4,00	C	Q
445	23.3	3,00	C	Q
445	18.0	2,40	C & Q	Q & C
405	25.6	3,00	C	Q
405	24.5	3,30	C	Q
395	26.8	5,30	C	Q
375	22.2	6,30	C	Q & C
370	14.0	3,10	C	Q
360	21.1	4,00	C	Q & C
350	19.8	6,30	C	Q
350	16.0	4,30	C	Q & C
320	10.0	5,00	Q	Q
300	18.0	8,40	C & Q	Q
285	26.1	7,40	C	Q & C
265	29.1	6,30	C	Q
265	23.1	9,00	C	Q
215	18.0	5,00	C	Q
215	14.0	20,00	C	Q
210	14.0	5,40	Q	Q
210	10.0	20,40	Q	Q
185	20.0	5,00	C	Q

Q : quartz   C : coesite

(i) *P–T equilibrium relationship between quartz and coesite.*

The conditions of pressure and temperature under which the experiments were carried out are listed in Table 2. The magnitude of the pressure in this Table was calculated from the ratio of the load pressure to the area of the anvil, and the temperature was measured by Pt–PtRd thermo-couple. The line (1) in Fig. 1 illustrates the P–T equilibrium relationship between quartz and coesite obtained directly from the present experiment. However,
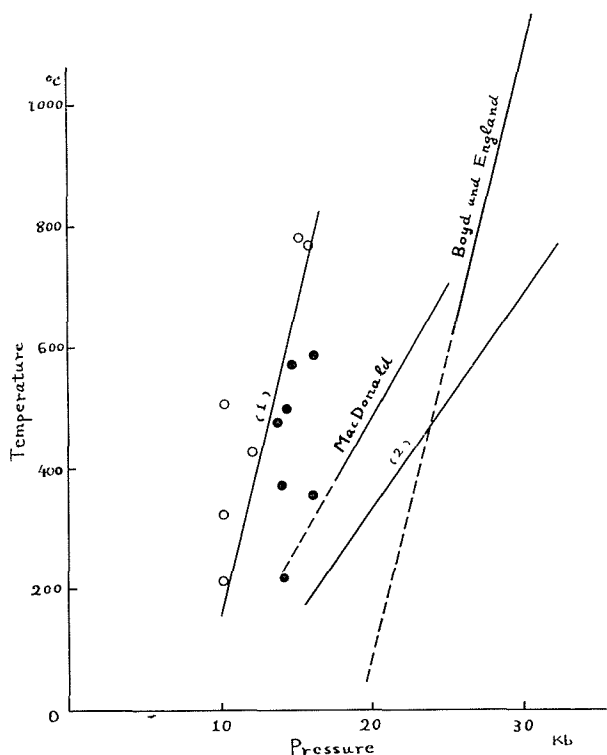

Fig. 1. P–T equilibrium relationship between quartz
and coesite.

the actual pressure acting on the specimen should not be represented by the ratio of the load pressure to the area of the anvil by the configuration shown in Part I. If this configuration is taken into account, the new equilibrium curve is drawn as shown by the line (2) in the same diagram; this curve being represented by the equation $P = 10.5 + 0.025T$.

(ii) *Stability of coesite.*

Coes reported that the new dense polymorph of silica synthesized by him

was "so stable that, once formed, any measurement on the reverse trans-
formation was impossible". Regarding the stability of coesite, a number of
runs were carried out also by the present author in the temperature range
up to 1100°C under the ordinary pressure. No recognizable changes were
found even with extending heating over 2 weeks. After these unsuccessful
runs to convert coesite to quartz at the ordinary pressure, experiments were
carried out at some P–T conditions in quartz region. The starting material
was the 1 to 1 mixture of silica gel and pulverized coesite. The mixture
was covered with gold foil as mentioned in the preceding section and placed
under some P–T condition for a few hours. Plate 8 shows the photographs
of X–ray diffraction pattern of some of these runs. The top one of the
Plate was the photograph of the run at 1 bar 400°C for 4 hours. The distinct
lines of both quartz and coesite are able to be distinguished in this picture.
The second one was that at 15 kb 400°C for 4 hours, and there may be found
far more distinct lines of quartz than that of coesite. From the fact shown
by these photographs, it may be reasonably considered that coesite is con-
vertible to quartz under the proper P–T conditions rather in short time.
These P–T conditions are not so high as unable to be expected in the earth's
crust.

Discussion on the natural occurrence of coesite

It seems probable that the P–T condition at the boundary region between
the crust and the mantle of the earth can be high enough to transform
quartz to coesite, or that P–T condition making this transformation possible
exists in nature, especially in the region metamorphosed in high-grade. If
coesite is very stable, the rocks produced at the above-mentioned condition
should contain some coesite in them. In spite of many efforts to find out
coesite in nature, there have been no reports informing the existence of coesite
crystals in natural rocks except for some from meteor craters and also from
pits produced by explosions of atomic bombs[14]. To explain this fact the
following two cases are considered. (1) P–T condition which is favorable to
produce coesite does not exist either in the deep part of the crust or in the
metamorphosed region. (2) Coesite is not so stable as COES mentioned, and
has converted into quartz during geological time or under some P–T con-
ditions.

MACDONALD pointed out[7] that the quartz-coesite boundary determined
by him lay about 30 km above graphite-diamond transition boundary below
the earth's surface and therefore, coesite should be found in eclogite in
which diamond crystallized. But there were no report as to the discovery
of coesite in the eclogite. On the basis of their P–T relation, BOYD and
ENGLAND[9] deduced that the pressure in the crust was too low to form coesite
but in the mantle it was sufficient, so that we could hardly find coesite in
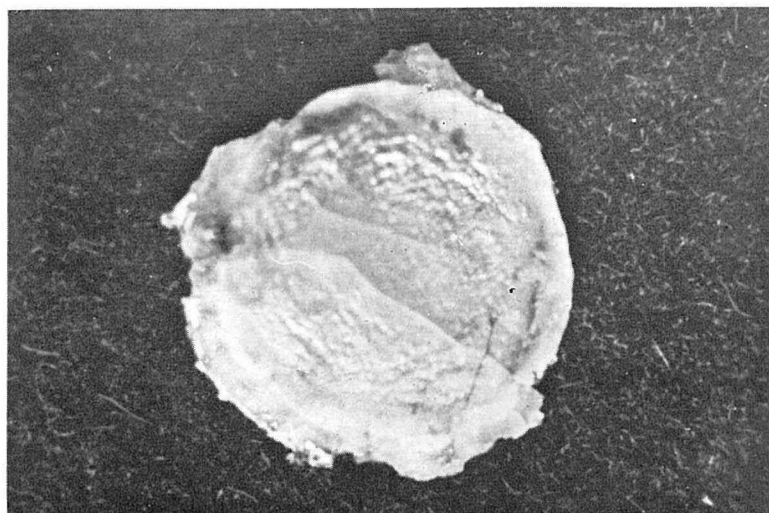
nature. The experimental data obtained under uni-directional compression, however, show the possibility of the formation of coesite even at the depth of about 50 km in the crust. Moreover it seems probable that these conditions must have existed at the time of high-grade regional metamorphism where a uni-directional compression would prevail. Therefore, coesite must have been produced in the regional metamorphosed rock, provided that rocks were oversaturated with SiO_2, but as the P–T condition of metamorphosed rock gradually swerved from that of coesite-stable region, coesite once produced must have transformed into quartz.
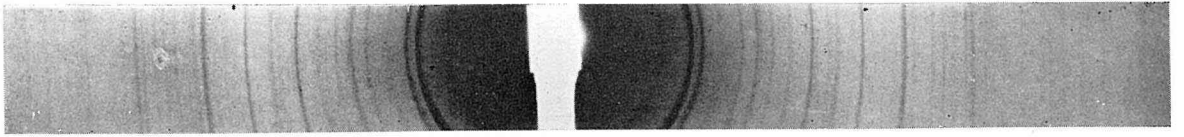
Acknowledgments

References

1) COES, L., Jr. : Science, 118, p. 131 (1953).
2) SOSMAN, R. B. : Science, 119, p. 738 (1954).
3) RAMSDELL, L. S. : Am. Mineralogist, 40, p. 975 (1955).
4) ZOLTAI, T. and M. J. BUERGER : Z. Krist., 111, p. 129 (1959).
5) KHITAROV, N. N., A. B. SLURSKIY and R. V. AREN'YEVA : Geokhimiya, 8, p. 666 (1957).
6) GRIGGS, D. T. and G. C. KENNEDY : Am. J. Sci., 254, p. 722 (1956).
7) MACDONALD, G. J. F. : Am. J. Sci., 254, p. 713 (1956).
8) HALL, H. T. : Rev. Sci. Instrument, 31, p. 126 (1960).
9) BOYD, F. R. and J. L. ENGLAND : J. Geophys. Research, 65, p. 749 (1960).
10) HALL, H. T. : Science, 128, p. 445 (1958).
11) VOLAROCICH, M. P. and E. I. PARKOMENKO : Bull. Acad. Sci. U.S.S.R., Geophysics series, no. 2, p. 69 (1957).
12) ZWIKKER, C. : Physical Properties of Solid Materials (1955).
13) HILL, R. : The Mathematical Theory of Plasticity (1950), in Japanese.
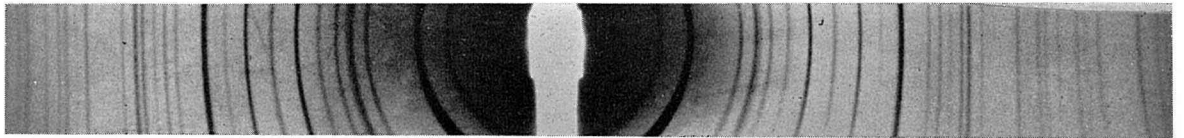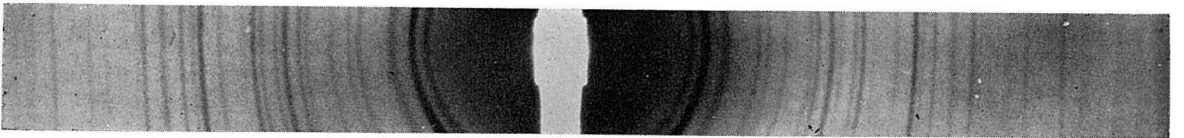14) PECOLA, W. T. : Geo. Times. 5, p. 16 (1960).

a

b

(1)

(2)

quartz

coesite